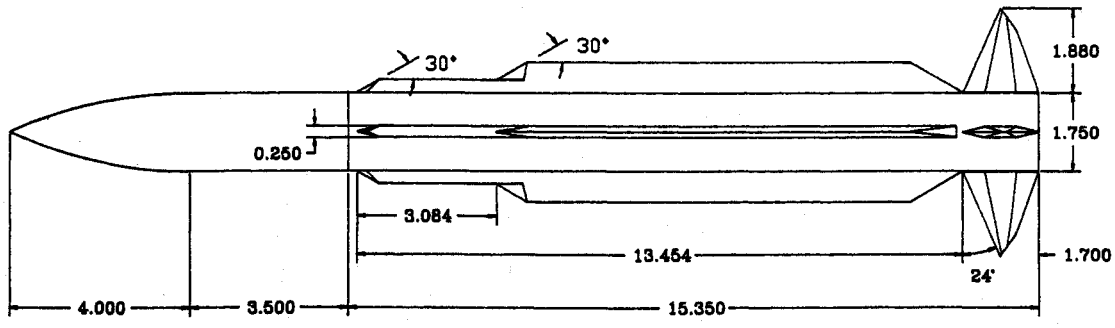


Fig. 1 VLSAM model (dimensions in inches).

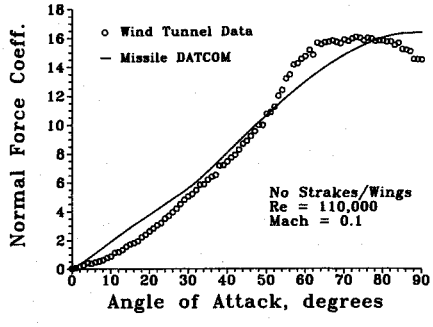


Fig. 2 Normal-force data and prediction—without strakes and wings.

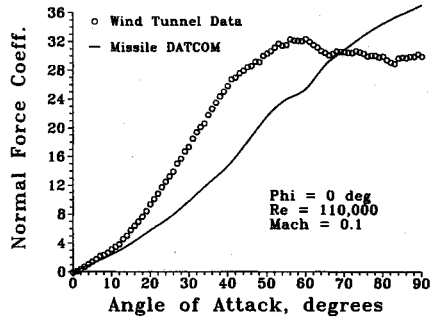


Fig. 3 Normal-force data and prediction—0-deg roll angle.

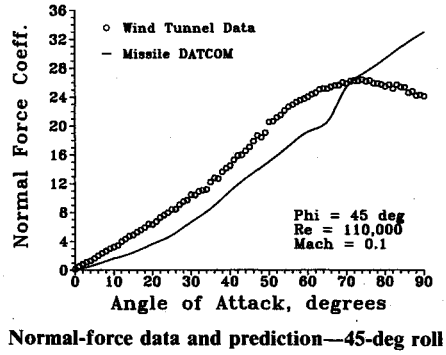


Fig. 4 Normal-force data and prediction—45-deg roll angle.

the specified margin allowable for preliminary design. However, as in the previous case, the experimental values of $C_N$ fall off at higher angles while the predicted values tend to continue increasing. The curves for both roll angles cross at 70 deg.

To summarize, for the case studied, Missile DATCOM was found to predict normal-force behavior very well for the body-tail configuration, up to extremely high angles of attack. Poorer correlation was found to exist for the complete configuration at roll angles of 0 and 45 deg. A method better than can be achieved from extrapolated aircraft data must be developed to treat unconventional wing planforms.

## Acknowledgments

The authors wish to thank the personnel of the W. R. Church Computer Center at the Naval Postgraduate School for their assistance, and also the personnel involved with Missile DATCOM at the Flight Dynamics Laboratory, Wright Patterson Air Force Base, for their assistance in obtaining a copy of and documentation for the computer program.

## References

[1]Vukelich, S. R., Stoy, S. L., Burns, K. A., Castillo, J. A., and Moore, M. E., "Missile DATCOM Volume I—Final Report," Air Force Wright Aeronautical Lab., Wright Patterson AFB, OH, AFWAL-TR-86-3091, Dec. 1988.

[2]Hoak, D. E., Carlson, J. W., and Malthan, L. V. (eds.), "USAF Stability and Control DATCOM," Air Force Wright Aeronautical Lab., Wright Patterson AFB, OH, AFWAL-TR-83-3098, Oct. 1960, revised 1978.

[3]Howard, R. M., Rabang, M. P., and Roane, D. P., Jr., "Aerodynamic Effects of a Turbulent Flowfield on a Vertically Launched Missile," *Journal of Spacecraft and Rockets,* Vol. 26, No. 6, 1989, pp. 445–451.

[4]Dunne, A. L., Black, S., Schmidt, G. S., and Lewis, T. L., "VLA Missile Development and High Angle of Attack Behavior," *Proceedings of the NEAR Conference on Missile Aerodynamics,* Monterey, CA, Oct. 31–Nov. 2, 1988, pp. 13-1–13-68.

Walter B. Sturek
*Associate Editor*

# Flight Stagnation-Point Heating Calculations on Aeroassist Flight Experiment Vehicle

H. H. Hamilton II,* Roop N. Gupta,† and Jim J. Jones‡
*NASA Langley Research Center, Hampton, Virginia 23665*

## Nomenclature

$q$ = wall heating rate, kW/m$^2$
$R$ = nose radius, m
$T$ = temperature, K

Received April 26, 1990; revision received July 30, 1990; accepted for publication Aug. 3, 1990. 

*Research Engineer. Member AIAA.

†Research Scientist, Scientific Research and Technology, Inc., Hampton, VA 23693. Associate Fellow AIAA.

‡Senior Engineer, Analytical Mechanics Associates, Hampton, VA 23666.

$V_\infty$ = freestream velocity, km/s
$\epsilon$ = tile emissivity
$\sigma$ = Stefan-Boltzman constant, $5.6696 \times 10^{-14}$ $MW/m^2K^4$
$\rho$ = density, $kg/m^3$

*Subscripts*

$c$ = convective
eff = effective
$r$ = radiative
req = radiation equilibrium
sp = stagnation point
$w$ = wall
$\infty$ = freestream

## Introduction

IN order to obtain the data necessary to design future aeroassisted space transfer vehicles, NASA is currently developing the Aeroassist Flight Experiment (AFE). This vehicle will be deployed from the Shuttle Orbiter (scheduled for 1994), make a data-gathering aeropass through the upper atmosphere, and then return to orbit for pickup by the shuttle. The primary purpose of the AFE is to obtain data in the flight regime where chemical and thermal nonequilibrium effects dominate the shock layer, because such effects may play a large role in the design of aeroshells for future aeroassisted space transfer vehicles. A review of aeroassist concepts is given by Walberg.[1]

The absence of applicable flight data and the inability of ground-based wind tunnels to simulate the low-density, high-energy flight environment[2,3] are the impelling forces that dictate the need for the AFE flight experiment. This lack of data also creates an uncertainty in the heat transfer predictions needed to design the AFE heat shield. Among the important factors that must be considered in the heating predictions are both chemical and thermal nonequilibrium, an extensive viscous region, small but finite wall recombination rates, nonequilibrium radiative heating, and three-dimensional effects due to a nonaxisymmetric heat shield geometry.

Rochelle and co-workers[4,5] have used an axisymmetric chemically reacting version of the BLIMP (boundary-layer integral matrix procedure) code[6] to predict AFE heating. In the present paper, an axisymmetric chemically reacting viscous-shock-layer code[7] has been used to calculate heating rates on the AFE. The present method of analysis automatically accounts for the viscous-inviscid interaction and entropy-layer-swallowing effects that are not properly accounted for in a classical boundary-layer method. The current method has been compared with a full three-dimensional Navier-Stokes code[8] for verification. Calculations of the stagnation point heating for the current AFE baseline trajectory are presented. Results for the high-altitude portion of the trajectory have also been calculated using the stagnation-region Navier-Stokes method described in Ref. 9.

## Vehicle and Trajectory

The aerobrake on the AFE vehicle (Fig. 1) is an elliptic cone, blunted with an ellipsoidal nose, and raked off at an angle of 17 deg relative to the cone axis. The ellipticity of the cone is such that it produces a circular base in the rake plane. This results in a highly three-dimensional stagnation region. A skirt is fitted tangent to the elliptic cone at the rake plane to reduce heating in this region. The aerobrake is made of a conventional aluminum structure covered with a thermal protection system, with the outer layer consisting of tiles similar to those used on the Shuttle Orbiter.[3]

The vehicle is deployed from the shuttle payload bay. It is maneuvered to its entry attitude and then driven into the outer fringes of the atmosphere at a high velocity by a solid rocket motor that is jettisoned prior to the data-collection phase of the experiment. The vehicle enters the atmosphere at approximately 9.9 km/s and penetrates to a perigee of approximately 75 km where its velocity has decreased to 8.6 km/s (see the baseline trajectory presented in Fig. 2). It is then maneuvered back into a higher Earth orbit using aerodynamic lift and is retrieved by the Shuttle Orbiter and returned to Earth. The most important part of the mission, from a scientific viewpoint, is the entry phase from 90 km down to 75 km where several instruments will take data.[3]

## Analysis

The stagnation region of the AFE vehicle is subjected to high heating on the entry phase of the mission prior to perigee. In order to design a vehicle that can survive and perform its mission successfully, one must accurately predict the stagnation-region heating environment. The conditions are such that the flow within the shock layer is in both thermal and chemical nonequilibrium. The surface heating is primarily convective, but the nonequilibrium radiative heating is too large to ignore completely.

Gnoffo[8] has developed a Navier-Stokes flowfield code, LAURA (Langley Aerothermodynamic Upwind Relaxation Algorithm), which uses a two-temperature thermal model and an 11-species chemical model. It has been applied to calculate the flowfield over the AFE vehicle in flight. In principle, this code could have been used in the present analysis to predict the convective stagnation-point heating rates; however, this would have required several hours of computer time on a CRAY-2 for each trajectory point. Instead, an axisymmetric viscous-shock-layer (VSL) code developed by Gupta[7] that uses a single-temperature thermal model and a 5-species chemical model has been employed. The VSL code requires much less computer time than the LAURA code (only 1 or 2 min per case), but it automatically accounts for viscous-inviscid interaction and is thus more accurate than a boundary-layer

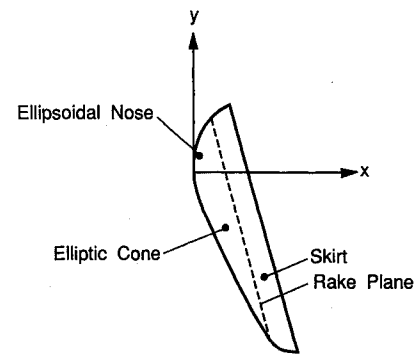


**Fig. 1 Geometry of AFE aerobrake.**

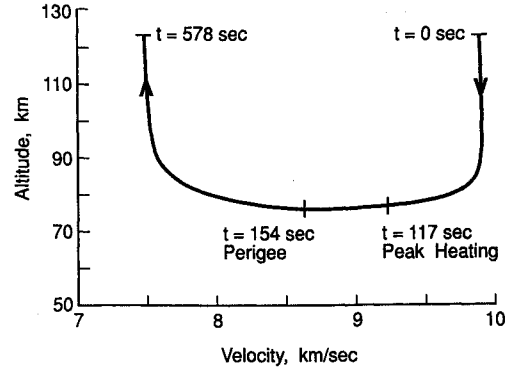


**Fig. 2 AFE baseline trajectory.**

method applied at these conditions. Although more sophisticated thermal and chemical models similar to those used in the LAURA code are required to properly account for nonequilibrium radiation,[10] the much simpler models used in the VSL code should be sufficiently accurate for calculating surface phenomena such as convective heating. The three-dimensional stagnation region of the AFE will be approximated by a sphere in the VSL code with an effective radius ($R_{\text{eff}}$) that produces the same heating rate as the LAURA code applied to the actual AFE vehicle at the peak heating point on the trajectory. By using this approach, the effective radius, $R_{\text{eff},c}$ of the sphere for the convective heating calculations was determined to be 2.16 m. For higher altitudes, where the low-density effects are more significant, the stagnation-region Navier-Stokes (SRNS) code[9] for an 11-species chemical model with and without wall-slip boundary conditions has been used. Similar to the VSL code, an effective radius has been used in the SRNS calculations. However, unlike the VSL code (which is based on shock fitting), the SRNS code captures the shock and thus automatically includes the effects of shock slip.

The surface of the aerobrake is covered with tile, made from the same material as that used on the Shuttle Orbiter, which has a small but finite chemical recombination rate. To account for this effect, the surface catalysis results of Stewart[11] have been used in the present calculations. The thermodynamic and transport properties used in the LAURA, VSL, and SRNS codes are the same and are described in Ref. 12.

Park[10] has developed a method to compute the nonequilibrium radiative stagnation-point heating rate on the AFE vehicle; however, this approach also requires a large amount of computer time (up to an hour to compute the stagnation point). To alleviate this problem, Jones (one of the present authors) developed the following correlation that matches Park's calculations to within approximately 10% for the conditions encountered by the AFE vehicle, with the largest deviations occurring at the higher altitudes. Following this approach, the approximate nonequilibrium radiative stagnation-point heating rate is given by the equation

$$\log (q_{w,r}) = 0.3542 + 0.5646V_\infty + (0.306 + 0.066V_\infty) \times \log (\rho_\infty R_{\text{eff},r}) \quad (1)$$

This equation was developed for use with trajectory calculations for the AFE and should be sufficiently accurate for the present analysis. The effective radius for the radiative heating calculation $R_{\text{eff},r}$ used in Eq. (1) is the nose radius, which provides the proper shock-layer thickness. This was obtained by matching the shock stand-off distance from the VSL calculation over a sphere to that predicted by the LAURA code on the actual AFE vehicle at the peak heating point on the trajectory. With this approach, the effective radius for the radiative heating $R_{\text{eff},r}$ was determined to be 2.74 m.

The wall temperature used in the present analysis was the radiation equilibrium value $T_{w,\text{req}}$ iteratively calculated from the following equation:

$$T_{w,\text{req}} = [(q_{w,c} + q_{w,r})/\epsilon\sigma]^{1/4} \quad (2)$$

where the surface emissivity $\epsilon$ was assumed to be 0.85.

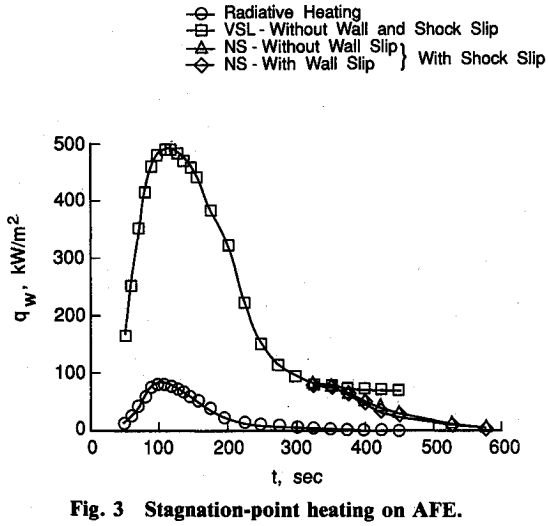


**Fig. 3 Stagnation-point heating on AFE.**

## Discussion of Results

By using the previously outlined approach, the stagnation-point heating rates for conditions along the AFE trajectory have been calculated and are presented in Fig. 3. The free-stream conditions used correspond to the project's baseline trajectory as of this writing, which is designated the baseline 5 mean trajectory. Peak total heating occurs at approximately 117 s (76 km) and produces a radiative equilibrium wall temperature of approximately 1785 K, which is near the upper limit of the surface tile. Peak radiative heating occurred slightly earlier and is only approximately 15% of the total heating.

For times greater than 325 s where the altitude is above 90 km, the heating rates calculated by the VSL code level off. In this region, the atmospheric density is reduced greatly compared with the perigee value, and the VSL equations are no longer completely valid. For the higher altitudes, heating calculations have been made using the SRNS code with and without wall slip. The heating rates obtained from this code match the VSL results at the lower altitude and decrease with increasing altitude as would be expected. For these conditions, including wall slip has little effect on the heating rates. The shock slip, which is automatically accounted for in the SRNS calculations with shock capturing, seems to impact the heating rates more significantly. Similar effects would be expected on the entry leg of the trajectory at high altitudes ($t < 50$ s in Fig. 3), but these calculations are not included in the present paper.

## Concluding Remarks

The results of these calculations represent the most complete and accurate set of continuum stagnation-point heating rates that have been obtained over the high heating portion of the AFE trajectory. They are currently being used in conjunction with nonequilibrium BLIMP calculations[2,3] to define the aerothermodynamic environment needed for the heat shield design.

## References

[1]Walberg, G. D., "A Survey of Aeroassisted Orbit Transfer," *Journal of Spacecraft and Rockets,* Vol. 22, Jan.-Feb. 1985, pp. 3-8.

[2]Jones, J. J., "The Rationale for an Aeroassist Flight Experiment," AIAA Paper 87-1508, June 1987.

[3]Walberg, G. D., Siemers, P. M., III, Calloway, R. L., and Jones, J. J., "The Aeroassist Flight Experiment," *Proceedings of the 38th International Astronautical Federation Congress,* Paper IAF-87-197, Oct. 1987.

[4]Rochelle, W. C., Ting, P. C., Mueller, S. R., Colovin, J. E., Bouslog, S. A., Curry, D. M., and Scott, C. D., "Aerobrake Heating Rate Sensitivity Study for the Aeroassist Flight Experiment (AFE)," AIAA Paper 89-1733, June 1989.

[5]Rochelle, W. C., Ting, P. C., Mueller, S. R., and Colovin, J. E., "Data Book Documentation, AFE Aerobrake Aerothermodynamic Data Book for Baseline V Trajectory, Volume I—Pitch Plane and Volume II—Off Pitch Planes," LESC-26950 (JSC-23623), Lockheed Engineering & Sciences Co., Houston, TX, April 1989.

[6]Tong, H., "User's Manual, Nonequilibrium Chemistry Boundary Layer Integral Matrix Procedure," Aerotherm Rept. UM-73-37, Part I, Aerotherm Corporation, Mountain View, CA, July 1973.
[7]Gupta, R. N., and Simmons, A. L., "Stagnation Flowfield Analysis for an Aeroasist Flight Experiment Vehicle," AIAA Paper 88-2613, June 1988.
[8]Gnoffo, P. A., "A Code Calibration Program in Support of the Aeroassist Flight Experiment," AIAA Paper 89-1673, June 1989.
[9]Gupta, R. N., "Navier-Stokes and Viscous Shock-Layer Solutions for Radiating Hypersonic Flows," AIAA Paper 87-1576, June 1987.
[10]Park, C., "Assessment of Two-Temperature Kinetic Model for Ionizing Air," AIAA Paper 87-1574, June 1987.
[11]Stewart, D. A., and Kolodziej, P., "Wall Catalysis Experiment on AFE," AIAA Paper 88-2674, June 1988.
[12]Gnoffo, P. A., Gupta, R. N., and Shinn, J. L., "Conservation Equations and Physical Models for Hypersonic Air Flows in Thermal and Chemical Nonequilibrium," NASA Tech. Paper 2867, Feb. 1989.

James E. Daywitt
*Associate Editor*